




## PAPER

[View Article Online](#)  
[View Journal](#) | [View Issue](#)

Cite this: *J. Mater. Chem. B*, 2021, 9, 7713

# pH-Sensitive branched $\beta$ -glucan-modified liposomes for activation of antigen presenting cells and induction of antitumor immunity†

Shin Yanagihara, Nozomi Kasho, Koichi Sasaki,  Naoto Shironaka, Yukiya Kitayama,  Eiji Yuba \* and Atsushi Harada\*

Induction of cellular immunity is important for effective cancer immunotherapy. Although various antigen carriers for cancer immunotherapy have been developed to date, balancing efficient antigen delivery to antigen presenting cells (APCs) and their activation via innate immune receptors, both of which are crucially important for the induction of strong cellular immunity, remains challenging. For this study, branched  $\beta$ -glucan was selected as an intrinsically immunity-stimulating and biocompatible material. It was engineered to develop multifunctional liposomal cancer vaccines capable of efficient interactions with APCs and subsequent activation of the cells. Hydroxy groups of branched  $\beta$ -glucan (Aqua $\beta$ ) were modified with 3-methylglutaric acid ester and decyl groups, respectively, to provide pH-sensitivity and anchoring capability to the liposomal membrane. The modification efficiency of Aqua $\beta$  derivatives to the liposomes was significantly high compared with linear  $\beta$ -glucan (curdlan) derivatives. Aqua $\beta$  derivative-modified liposomes released their contents in response to weakly acidic pH. As a model antigenic protein, ovalbumin (OVA)-loaded liposomes modified with Aqua $\beta$  derivatives interacted efficiently with dendritic cells, and induced inflammatory cytokine secretion from the cells. Subcutaneous administration of Aqua $\beta$  derivative-modified liposomes suppressed the growth of the E.G7-OVA tumor significantly compared with curdlan derivative-modified liposomes. Aqua $\beta$  derivative-modified liposomes induced the increase of CD8<sup>+</sup> T cells, and polarized macrophages to the antitumor M1-phenotype within the tumor microenvironment. Therefore, pH-sensitive Aqua $\beta$  derivatives can be promising materials for liposomal antigen delivery systems to induce antitumor immune responses efficiently.

Received 9th April 2021,  
Accepted 1st September 2021

DOI: 10.1039/d1tb00786f

[rsc.li/materials-b](https://rsc.li/materials-b)

## 1. Introduction

Cancer immunotherapy has gained much attention as a promising therapeutic approach for cancers since the success of immune checkpoint inhibitors.<sup>1</sup> To obtain therapeutic effects against cancers, the induction and activation of cell-based immunity (cellular immunity) are crucially important because cytotoxic T lymphocytes (CTLs) attack antigen-expressing tumor cells directly and specifically.<sup>2,3</sup> However, cancer-specific CTLs are not induced effectively in most patients. In addition, the CTL activity is suppressed in immunosuppressive microenvironments of tumor tissues.<sup>4</sup> Therefore, engineering approaches are desired to control the

immune responses artificially for the induction of cellular immunity and to cancel immunosuppressive environments within tumors.

To induce cancer-specific cellular immunity, exogenous antigens should be presented onto major histocompatibility complex (MHC) class-I molecules of antigen presenting cells (APCs) in a process designated as “cross-presentation”.<sup>5–7</sup> For induction of cross-presentation, the control of antigen delivery processes, such as antigen uptake by endocytosis through specific receptors expressed on APCs (such as mannose receptors) and cytosolic transport of antigens, is extremely important.<sup>5–8</sup> Cytosolic release of antigens can be achieved by mimicking viral entry into cells using membrane fusion with the plasma membrane or endosomal membrane.<sup>9,10</sup> To date, various virus-derived fusogenic protein-based or synthetic molecule-based membrane fusion systems have been developed to achieve efficient cytosolic delivery of antigens.<sup>9,10</sup>

In addition to the control of antigenic intracellular pathways, activation of innate immune pathways is crucially important to

Department of Applied Chemistry, Graduate School of Engineering, Osaka Prefecture University, 1-1 Gakuen-cho, Naka-ku, Sakai, Osaka 5998531, Japan.  
E-mail: [yuba@chem.osakafu-u.ac.jp](mailto:yuba@chem.osakafu-u.ac.jp), [harada@chem.osakafu-u.ac.jp](mailto:harada@chem.osakafu-u.ac.jp);  
Fax: +81-72-254-9330; Tel: +81-72-254-9330

† Electronic supplementary information (ESI) available. See DOI: 10.1039/d1tb00786f

induce antigen-specific cellular immunity. For example, when pathogens invade the body, dendritic cells (DCs) are activated *via* pattern recognition receptors such as toll-like receptors (TLRs) to induce adaptive immunity against pathogens effectively.<sup>11–15</sup> Importantly, activated DCs decrease the uptake capability of antigens.<sup>16,17</sup> Therefore, to induce antigen-specific immune response effectively, it is desirable to accumulate antigen delivery functions and adjuvant functions for the activation of innate immunity into a single carrier. However, precise control of antigen delivery processes and adjuvant functions using artificial immunity-inducing system remains challenging because the intracellular fate of both antigen and adjuvant molecules should be controlled accurately to achieve a cooperative effect.

We have previously synthesized various carboxylated polyglycidols or polysaccharides and modified them onto antigen-loaded liposomes to achieve cytosolic release of antigens within APCs.<sup>18–21</sup> Carboxylated polyglycidols or polysaccharides possess a hydrophobic nature after protonation of carboxy groups at acidic pH, which induced destabilization of liposomal and endosomal membranes after internalization to the cells, leading to cytosolic delivery of the antigen.<sup>18–21</sup> In addition, carboxylated polyglycidols with a hyperbranched structure were found to have enhanced liposome uptake by DCs compared with carboxylated polyglycidols having a linear structure.<sup>19</sup> This finding suggests that the bulky branched backbone structure of polymers can improve interactions with immune cells. Curdlan, a linear  $\beta$ -glucan, is known to induce the activation of APCs *via* recognition by Dectin-1 on DCs and macrophages.<sup>22,23</sup> We demonstrated that liposomes modified with 3-methylglutarylcurdlan (MGlu-Curd-A, Fig. 1) can deliver model antigens into the cytosol of DCs and thereby induce activation of these cells.<sup>24</sup> After subcutaneous injection to tumor-bearing mice, ovalbumin (OVA)-loaded, MGlu-Curd-A-modified liposomes induced OVA-specific cellular immunity and tumor regression more effectively than OVA-loaded liposomes modified with either 3-methylglutarylcurdlan or mannan.<sup>24</sup>

The backbone structure of carboxylated polymers dramatically affects multiple aspects of liposome-based antigen delivery systems such as cellular uptake, activation of innate immunity and adaptive immunity. Based on our previous observations revealing that hyperbranched polyglycidol derivatives demonstrated superior performance compared with their linear counterparts, here we sought to use  $\beta$ -glucan “Aqua $\beta$ ” (Fig. 1) instead of curdlan to develop a liposome-based antigen delivery system with

further enhanced therapeutic effects. Aqua $\beta$  has a branched structure. It is known to promote the secretion of inflammatory cytokines from APCs.<sup>25–27</sup> We synthesized MGlu unit-introduced Aqua $\beta$  derivatives and evaluated the therapeutic potential of Aqua $\beta$  derivative-modified liposomes containing OVA both *in vitro* and *in vivo*. The results show that the difference in the backbone structure of  $\beta$ -glucan increased the modification efficiency of polysaccharide derivatives to the liposomes and improved the immunity-inducing functions considerably, especially in the infiltration of CD8<sup>+</sup> cells into tumor tissue and the modulation of the macrophage composition in a tumor microenvironment.

## 2. Materials and methods

### 2.1. Materials

$\beta$ -1,3-1,6-Glucan (Aqua $\beta$ , Mw: 100 kDa, the degree of branching is 0.71 calculated from <sup>1</sup>H NMR) was kindly donated by Osaka Soda Co., Ltd (Osaka, Japan). Egg yolk phosphatidylcholine (EYPC) was kindly donated by NOF Co. (Tokyo, Japan). 3-Methylglutaric anhydride, curdlan from *Alcaligenes faecalis* (Mw: 294 kDa), ovalbumin (OVA), fetal bovine serum (FBS), *p*-xylene-bis-pyridinium bromide (DPX), DNase I, and dextran sulfate sodium salt from *Leuconostoc spp.* were purchased from Sigma-Aldrich (St. Louis, MO.). Collagenase D was obtained from Roche (Basel, Switzerland). 1-Aminodecane, pyranine and Triton X-100 were obtained from Tokyo Chemical Industries Ltd (Tokyo, Japan). 4-(4,6-Dimethoxy-1,3,5-triazin-2-yl)-4-methyl morpholinium chloride (DMT-MM), phenol and phospholipid C test-Wako were obtained from Wako Pure Chemical Industries Ltd (Osaka, Japan).

1,1'-Diocadecyl-3,3,3',3'-tetramethylindocarbocyanine perchlorate (DiI) was obtained from Life Technologies (Carlsbad, CA). Fixable Viability Dye eFluor<sup>®</sup> 520 was obtained from eBioscience (San Diego, CA). Sulfuric acid and calcium chloride (CaCl<sub>2</sub>) were obtained from nacalai tesque (Kyoto, Japan). The Coomassie (Bradford) Protein Assay Kit was obtained from Thermo Fisher Scientific K.K. (Tokyo, Japan). Sodium hydrogen carbonate was purchased from Kishida Chemical Co., Ltd (Osaka, Japan). Cellulose tubing for dialysis (MWCO: 12 000–14 000) was obtained from Viskase Companies, Inc. (Lombard, IL).

### 2.2. Synthesis of $\beta$ -glucan derivatives

3-Methylglutaryl Aqua $\beta$  (MGlu-Aqua $\beta$ ) and 3-methylglutarylcurdlan (MGlu-Curd) were prepared by reaction of Aqua $\beta$

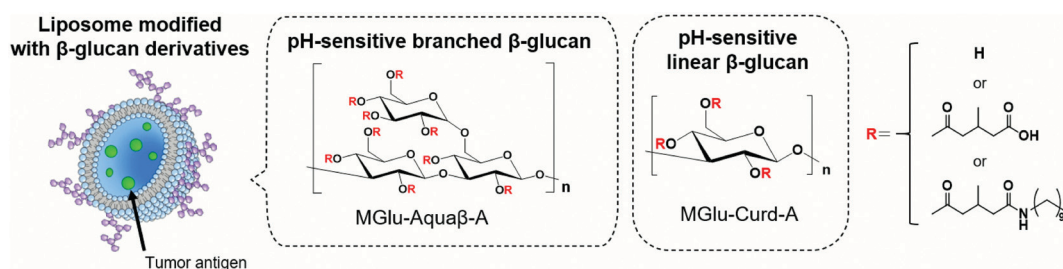


Fig. 1 Design of antigen-loaded liposomes modified with pH-sensitive  $\beta$ -glucan derivatives as cancer immunity-inducing systems.

and curdlan with 3-methylglutaric anhydride, respectively (Fig. S1 and Table S1, ESI†). A given amount of 3-methylglutaric anhydride shown in Table S1 (ESI†) was added to a *N,N*-dimethylformamide (DMF) solution of Aquaβ or curdlan and stirred at 90 °C for 24 h under a nitrogen atmosphere. Then, saturated sodium hydrogen carbonate aqueous solution was added to the reaction mixture for neutralization, and the reaction mixture was purified through a dialysis against water with a dialysis membrane (MWCO: 12 000–14 000) for 3 days. The product was collected by freeze-drying. <sup>1</sup>H NMR for hydrolyzed MGLu-Aquaβ (400 MHz, D<sub>2</sub>O + NaOD): δ 0.9 (d, *J* = 6.0 Hz, –CO–CH<sub>2</sub>–CH(CH<sub>3</sub>)–CH<sub>2</sub>–), 2.0 (dd, *J* = 9.9, 14.3 Hz, –CO–CH<sub>2</sub>–CH(CH<sub>3</sub>)–CH<sub>2</sub>–), 2.2–2.3 (m, –CO–CH<sub>2</sub>–CH(CH<sub>3</sub>)–CH<sub>2</sub>–), 3.2–4.3 (br, glucose 2H, 3H, 4H, 5H, 6H), 4.5 (d, *J* = 7.6 Hz, β1,6-linked 1H), 4.7–5.1 (m, HDO, β1,3-linked 1H)<sup>28</sup> (Fig. S2b, ESI†). <sup>1</sup>H NMR for hydrolyzed MGLu-Curd (400 MHz, D<sub>2</sub>O + NaOD): δ 0.9 (d, *J* = 6.0 Hz, –CO–CH<sub>2</sub>–CH(CH<sub>3</sub>)–CH<sub>2</sub>–), 2.0 (dd, *J* = 9.9, 14.3 Hz, –CO–CH<sub>2</sub>–CH(CH<sub>3</sub>)–CH<sub>2</sub>–), 2.2–2.3 (m, –CO–CH<sub>2</sub>–CH(CH<sub>3</sub>)–CH<sub>2</sub>–), 3.4–4.1 (br, glucose 2H, 3H, 4H, 5H, 6H), 4.7–5.1 (m, HDO, β1,3-linked 1H)<sup>29</sup> (Fig. S2c, ESI†).

As an anchor moiety for the fixation of MGLu-Aquaβ and MGLu-Curd onto liposome membranes, 1-aminodecane was combined with carboxy groups of MGLu-Aquaβ and MGLu-Curd. Each polymer was dissolved in water. A given amount of 1-aminodecane shown in Table S2 (ESI†) was reacted with the carboxy groups of the polymer using DMT-MM at room temperature for 24 h with stirring. The obtained polymers were purified through dialysis against water with a dialysis membrane (MWCO: 12 000–14 000) for more than 3 days until no water permeation within the dialysis membrane takes place. The product was recovered by freeze-drying. <sup>1</sup>H NMR for hydrolyzed MGLu-Aquaβ-A (400 MHz, D<sub>2</sub>O + NaOD): δ 0.8–1.0 (m, –CO–CH<sub>2</sub>–CH(CH<sub>3</sub>)–CH<sub>2</sub>–, CO–NH–CH<sub>2</sub>–(CH<sub>2</sub>)<sub>8</sub>–CH<sub>3</sub>), 1.1–1.7 (br, –CO–NH–CH<sub>2</sub>–(CH<sub>2</sub>)<sub>8</sub>–CH<sub>3</sub>), 2.0 (dd, *J* = 9.9, 14.3 Hz, –CO–CH<sub>2</sub>–CH(CH<sub>3</sub>)–CH<sub>2</sub>–), 2.2–2.3 (m, –CO–CH<sub>2</sub>–CH(CH<sub>3</sub>)–CH<sub>2</sub>–), 3.2–4.3 (m, glucose 2H, 3H, 4H, 5H, 6H), 4.5 (d, *J* = 7.6 Hz, β1,6-linked 1H), 4.7–5.1 (m, HDO, β1,3-linked 1H) (Fig. S2b, ESI†). <sup>1</sup>H NMR for hydrolyzed MGLu-Curd-A (400 MHz, D<sub>2</sub>O + NaOD): δ 0.8–1.0 (m, –CO–CH<sub>2</sub>–CH(CH<sub>3</sub>)–CH<sub>2</sub>–, CO–NH–CH<sub>2</sub>–(CH<sub>2</sub>)<sub>8</sub>–CH<sub>3</sub>), 1.1–1.7 (br, –CO–NH–CH<sub>2</sub>–(CH<sub>2</sub>)<sub>8</sub>–CH<sub>3</sub>), 2.0 (dd, *J* = 9.9, 14.3 Hz, –CO–CH<sub>2</sub>–CH(CH<sub>3</sub>)–CH<sub>2</sub>–), 2.2–2.3 (m, –CO–CH<sub>2</sub>–CH(CH<sub>3</sub>)–CH<sub>2</sub>–), 3.4–4.1 (m, glucose 2H, 3H, 4H, 5H, 6H), 4.5 (d, β1,6-linked 1H), 4.7–5.1 (m, HDO, β1,3-linked 1H) (Fig. S2c, ESI†).

### 2.3. Preparation of β-glucan derivative-modified liposomes

A given amount (5–10 mg) of EYPC dissolved in chloroform was added to a round-bottom flask. After evaporation of chloroform, β-glucan derivatives (lipid/polymer = 7/3, w/w) dissolved in methanol were added to the flask and the solvent was evaporated. The remaining organic solvent was further removed under vacuum. The obtained mixed thin film of EYPC and β-glucan derivatives was dispersed in phosphate-buffered saline (PBS) for the phenol-sulfuric acid method or OVA/PBS solution (4 mg mL<sup>−1</sup>) for other experiments by a brief sonication, and the liposome suspension was further hydrated by freezing and thawing and was extruded through a polycarbonate

membrane with a pore size of 200 nm. The liposome suspension was purified with ultracentrifugation for 1 h at 4 °C twice.

### 2.4. Characterization of liposomes

The diameters and zeta potentials of the liposomes (0.1 mM of lipid concentration) were measured using a Zetasizer Nano ZS (Malvern Instruments Ltd, Worcestershire, UK). Data were obtained as an average of more than three measurements on different samples.

The concentrations of the lipid and OVA in liposome suspension were measured using phospholipid C test-Wako and a Coomassie Protein Assay Reagent, respectively. Polysaccharide contents per lipid were measured by using a phenol-sulfuric acid method. To 200 μL aqueous solution of β-glucan derivative-modified liposomes, 200 μL of 5% phenol aqueous solution and 1 mL of 98% sulfuric acid were sequentially added. The mixture was vortexed and then incubated for 1 h. For a calibration curve, mixtures of 0–500 μg mL<sup>−1</sup> of β-glucan derivatives and EYPC suspension at an equal concentration to tested β-glucan derivative-modified liposomes were prepared. Absorption spectra (400–600 nm) for samples were measured and polysaccharide contents were calculated from the secondary differentiation of absorbance at 497 nm.

Pyranine-loaded liposomes were prepared as described above except that the mixture of polymer and EYPC was dispersed in aqueous 35 mM pyranine, 50 mM DPX, and 25 mM phosphate solution (pH 7.4). Liposomes encapsulating pyranine (lipid concentration: 2.0 × 10<sup>−5</sup> M) were added to PBS of varying pH at 37 °C and the fluorescence intensity at 512 nm of the mixed suspension was followed by excitation at 416 nm using a spectrofluorometer (Jasco FP-6500). The release percentage of pyranine from liposomes was defined as:

$$\text{Release (\%)} = (F_t - F_i) / (F_t - F_i) \times 100$$

where *F<sub>i</sub>* and *F<sub>t</sub>* mean the initial and intermediary fluorescence intensities of the liposome suspension, respectively. *F<sub>t</sub>* is the fluorescence intensity of the liposome suspension after the addition of Triton X-100 (final concentration: 0.1%).

### 2.5. Cellular association of liposomes

DiI-labeled liposomes were prepared as described above except that a mixture of polymer and lipid containing DiI (0.1 mol%) was dispersed in PBS containing OVA. DC2.4 cells, murine dendritic cell lines (7.5 × 10<sup>4</sup> cells) cultured for 2 days in a 24-well plate, were washed twice with HBSS and then incubated in serum-free medium (0.25 mL). DiI-labeled liposomes (1 mM lipid concentration, 0.25 mL) were added gently to the cells and then incubated for 4 h at 37 °C. After incubation, the cells were washed with HBSS three times. The fluorescence intensity of these cells was determined *via* a flow cytometric analysis (CytoFlex, Beckman Coulter, Inc.). The relative fluorescence intensity for each liposome was calculated using the fluorescence intensity of the cells treated with unmodified liposomes. For an inhibition assay, 10 μg mL<sup>−1</sup> dextran sulfate was pre-incubated with cells for an hour. Then, DiI-labeled liposomes

were added to the cells. After 4 h incubation, the fluorescence intensity of these cells was measured as described above.

## 2.6. Cytokine production from dendritic cell lines

DC2.4 cells ( $3 \times 10^5$  cells) cultured for 2 days in a six-well plate were washed with HBSS twice and then incubated in serum-free RPMI-1640 medium.  $\beta$ -glucan derivatives in PBS (final concentration:  $0.5 \text{ mg mL}^{-1}$ ) or OVA-loaded liposomes (final lipid concentration:  $0.5 \text{ mM}$  corresponding to  $0.4 \text{ mg mL}^{-1}$  lipid) were added gently to the cells, followed by incubation for 24 h at  $37^\circ\text{C}$ . After incubation, supernatants were collected, and cytokine (IL-12 and IL-1 $\beta$ ) production was measured using an enzyme-linked immunosorbent assay kit (ELISA Development Kit, PeproTech EC Ltd) according to the manufacturer's instruction.

## 2.7. Mice

Seven-week-old female C57BL/6 mice (H-2<sup>b</sup>) were purchased from Oriental Yeast Co., Ltd (Tokyo, Japan). All animal experiments were approved by the Institutional animal experimentation committee in Osaka Prefecture University (Approval No. 19-1, 20-1) and were performed in compliance with the institutional guidelines of animal care and use.

## 2.8. Induction of antitumor immunity

E.G7-OVA cells, OVA-expressing T-lymphoma ( $5.0 \times 10^5$  cells per mouse), were subcutaneously inoculated into the left back of C57BL/6 mice under anesthesia with isoflurane. On days 8 and 14,  $100 \mu\text{g}$  of OVA-loaded liposomes were subcutaneously injected into the right backs of the mice under anesthesia with isoflurane. Tumor sizes were monitored from the day of tumor inoculation. Mice immunized with PBS were used as a control to confirm the development of tumors following the first inoculation of E.G7-OVA cells. Mice were sacrificed when tumor volumes became over  $2000 \text{ mm}^3$ . All treated groups contained five mice.

## 2.9. Analysis of immune cell composition in the tumor

E.G7-OVA cells ( $5.0 \times 10^5$  cells per mouse) were subcutaneously inoculated into the left back of C57BL/6 mice under anesthesia with isoflurane. On day 6,  $100 \mu\text{g}$  of OVA-loaded liposomes were subcutaneously injected into the right backs of the mice under anesthesia with isoflurane. On day 12, mice were sacrificed and tumor tissues were excised. Tumors were cut into small pieces and digested by incubating in sodium pyruvate-free DMEM medium supplemented with  $1.2 \text{ mM CaCl}_2$ ,  $2 \text{ mg mL}^{-1}$  Collagenase D and  $0.04 \text{ mg mL}^{-1}$  DNase I at  $37^\circ\text{C}$  for 1 h. Single cell suspension of the tumor was prepared by gently mashing and passing through a  $70 \mu\text{m}$  mesh Cellstrainer<sup>TM</sup> (Falcon<sup>®</sup>). Erythrocytes were removed by incubating the cell pellet for 5 min in ammonium chloride buffer ( $7.47 \text{ mg mL}^{-1}$   $\text{NH}_4\text{Cl}$ ,  $2.06 \text{ mg mL}^{-1}$  tris(hydroxymethyl)aminomethane, pH 7.4) at  $4^\circ\text{C}$ . Tumor cells were seeded into 96-well plates with  $1.0 \times 10^6$  cells per well and washed with PBS. To discriminate between live and dead cells, the cells were incubated for 30 min on ice with Fixable Viability Dye eFluor<sup>®</sup> 520 (diluted 1:1000 in PBS), and washed with FACS buffer (PBS containing 2% FBS) twice.

The cells were incubated with  $5 \mu\text{g mL}^{-1}$  CD16/CD32 monoclonal antibody (eBioscience) for 20 min at  $4^\circ\text{C}$  to block Fc receptors, and then washed twice. To analyze T cell populations, the cells were stained with anti-CD8-PE (eBioscience, 53-6.7), anti-CD3 $\epsilon$ -PerCP-Cy5.5 (BD Bioscience, 145-2C11) and anti-CD4-PE/Cy7 (BD Bioscience, RM4-5) for 20 min at  $4^\circ\text{C}$ . For analysis of macrophage populations, the cells were stained with anti-CD206-PE (BioLegend, C068C2), anti-CD11b-PerCP-Cy5.5 (BD Pharmingen<sup>TM</sup>, M1/70) and anti-I-A<sup>b</sup>-PE/Cy7 (BioLegend, AF6-120.1) antibodies for 20 min at  $4^\circ\text{C}$  (each diluted 1:200 in FACS buffer). After washing twice, cell populations were analyzed *via* a flow cytometric analysis.

## 2.10. Statistical analysis

Statistically significant differences between experimental groups were determined using Prism software (v8, GraphPad) Where one-way ANOVA followed by Tukey's HSD *post hoc* test was used, variance between groups was found to be similar by the Brown-Forsythe test. The symbols \*, \*\*, \*\*\*, and \*\*\*\* indicate *P* values less than 0.05, 0.01, 0.001, and 0.0001, respectively.

# 3. Results

## 3.1. Synthesis of $\beta$ -glucan derivatives and modification onto the liposomes

Synthesis of pH-sensitive Aqua $\beta$  derivatives was performed as shown in Fig. S1 (ESI<sup>†</sup>), and Tables S1 and S2 (ESI<sup>†</sup>). Hydroxy groups of Aqua $\beta$  were reacted with 3-methylglutaric anhydrides to introduce carboxylic esters (MGLu groups). Decyl groups were further introduced *via* amide bonds as an anchor moiety to fix Aqua $\beta$  derivatives onto the liposomal membrane. pH-Sensitive curdlan derivatives were synthesized according to our previous report.<sup>24</sup> For <sup>1</sup>H NMR analysis of obtained compounds, broad peaks appeared corresponding to MGLu groups (0.9 and 1.9–2.3 ppm) and decyl groups (0.8–1.7 ppm) along with sugar moieties (3.2–4.7 ppm) (Fig. S2a, ESI<sup>†</sup>), indicating the introduction of MGLu groups and decyl groups into  $\beta$ -glucans. The percentages of MGLu groups (MGLu%) and anchor groups (anchor%) of  $\beta$ -glucan derivatives were calculated from the peak area ratio of sugar moieties and MGLu groups or decyl groups after hydrolysis by NaOD (Tables S2 and S3, Fig. S2b and S2b, ESI<sup>†</sup>). The  $\beta$ -glucan derivatives bearing various percentages of MGLu groups with comparable anchor% were successfully synthesized (Tables S1 and S2, ESI<sup>†</sup>). Each  $\beta$ -glucan derivative was designated as MGLuX-Curd-AY or MGLuX-Aqua $\beta$ -AY, where X and Y respectively represent MGLu% and anchor% per hydroxy groups. The MGLu and anchor densities per 100  $\beta$ 1,3-linked sugar units for both Aqua $\beta$  and curdlan derivatives were also calculated (Table S2, ESI<sup>†</sup>). The MGLu and anchor densities of Aqua $\beta$  derivatives were relatively high compared with those of curdlan derivatives because of MGLu and anchor groups introduced into the branched sugar units of Aqua $\beta$ .

Using hydration of a mixed thin film composed of EYPC and  $\beta$ -glucan derivatives, the  $\beta$ -glucan derivatives were introduced onto liposomes. Table 1 shows the size and zeta potentials of the prepared liposomes: all liposomes had 100–200 nm of

Table 1 Characterization of  $\beta$ -glucan derivative-modified liposomes

Liposome	Size (nm)	PDI	$\zeta$ -Potential (mV)	OVA/lipid ( $\text{g mol}^{-1}$ )	Encapsulation efficiency (%)
Unmodified	175 $\pm$ 15	0.17 $\pm$ 0.02	−7.90 $\pm$ 2.8	253 $\pm$ 96	39.6 $\pm$ 15
MGlu70-Aqua $\beta$ -A6	126 $\pm$ 14	0.23 $\pm$ 0.04	−42.3 $\pm$ 8.0	143 $\pm$ 43	22.4 $\pm$ 6.7
MGlu56-Aqua $\beta$ -A4	119 $\pm$ 3.1	0.20 $\pm$ 0.02	−42.3 $\pm$ 5.4	116 $\pm$ 19	18.1 $\pm$ 3.0
MGlu38-Aqua $\beta$ -A3	127 $\pm$ 13	0.17 $\pm$ 0.01	−46.0 $\pm$ 10	107 $\pm$ 25	16.7 $\pm$ 3.9
MGlu21-Aqua $\beta$ -A2	148 $\pm$ 21	0.25 $\pm$ 0.06	−40.1 $\pm$ 5.0	186 $\pm$ 8.8	29.1 $\pm$ 1.4
MGlu71-Curd-A6	210 $\pm$ 32	0.16 $\pm$ 0.08	−45.3 $\pm$ 2.4	111 $\pm$ 25	17.4 $\pm$ 3.9
MGlu62-Curd-A4	139 $\pm$ 27	0.21 $\pm$ 0.01	−31.0 $\pm$ 12	204 $\pm$ 2.5	31.9 $\pm$ 0.4
MGlu37-Curd-A4	154 $\pm$ 6.6	0.14 $\pm$ 0.02	−41.1 $\pm$ 3.4	114 $\pm$ 28	17.8 $\pm$ 4.4
MGlu13-Curd-A4	103 $\pm$ 8.0	0.17 $\pm$ 0.01	−27.6 $\pm$ 6.6	118 $\pm$ 10	18.5 $\pm$ 1.6

average size, corresponding to the pore size of polycarbonate membrane used for extrusion. It was confirmed by TEM observation that the liposome structure with a lipid bilayer was maintained even after the modification of  $\beta$ -glucan derivatives (Fig. S3, ESI†). Liposomes prepared from the mixture of EYPC and  $\beta$ -glucan derivatives exhibited large absolute values of negative zeta potentials compared with EYPC liposomes without polymer modification, suggesting that  $\beta$ -glucan derivatives were modified onto liposomal membranes. The amounts of  $\beta$ -glucan derivatives per lipid were evaluated using the phenol-sulfuric acid assay, which is a standard quantitative assay of sugar.<sup>30,31</sup> The modification efficiency of Aqua $\beta$  and curdlan derivatives were compared using  $\beta$ -glucan derivative-modified liposomes without OVA loading (Fig. 2). It was obvious that Aqua $\beta$  derivatives exhibit higher modification efficiency than curdlan derivatives, and this might be due to the difference in the anchor density of  $\beta$ -glucan derivatives (Table S2, ESI†).  $\beta$ -glucan derivatives with relative high anchor density, *i.e.* Aqua $\beta$  derivatives, were fixed to liposomes with high efficiency. As a model antigenic protein, OVA was

encapsulated into each liposome. The amounts of OVA per lipid ( $\text{g mol}^{-1}$ ) were 100–250 and the encapsulation efficiency of OVA was 17–40%, which is comparable with our previous reports using carboxylated chondroitin sulfate derivative-modified liposomes and carboxylated hyperbranched polyglycidols.<sup>21,32</sup>

Destabilization of Aqua $\beta$  derivative-modified liposomes in response to a decrease in pH to acidic pH was evaluated using liposomes encapsulating both a fluorescent dye (pyranine) and its quencher (DPX). The increase in fluorescence intensity derived from pyranine released from the liposomes at varying pHs was monitored (Fig. 2). Although the release of pyranine from unmodified EYPC liposomes never exceeded 20% of the total amounts in any evaluated pH range, Aqua $\beta$  derivative-modified liposomes could release pyranine in response to acidic pH in the same way as that with curdlan derivative-modified liposomes (Fig. 3 and Fig. S4, S5, ESI†).

### 3.2. Adjuvant properties of Aqua $\beta$ derivative-modified liposomes and their cellular interaction

Adjuvant effects of Aqua $\beta$  derivatives without modification onto liposomes were evaluated and compared with those of curdlan derivatives by measuring secretions of inflammatory cytokines from the dendritic cell line (DC2.4 cell) (Fig. 4a and b). After 24 h incubation of DC2.4 cells with  $\beta$ -glucan derivatives, inflammatory cytokines in a cell culture supernatant were quantified by ELISA assay. Aqua $\beta$  with high MGlu% (MGlu63, 75) induced significantly higher amounts of IL-12 and IL-1 $\beta$  secretion than parental Aqua $\beta$  and Aqua $\beta$  derivatives with low MGlu%, although there was no clear correlation between cytokine production and MGlu% for curdlan derivatives. In particular, MGlu75-Aqua $\beta$  showed significantly high IL-1 $\beta$  secretion compared with the other  $\beta$ -glucan derivatives. Adjuvant effects of liposomes modified with  $\beta$ -glucan derivatives were also evaluated (Fig. 4c and d). In both IL-12 and IL-1 $\beta$  secretions, significantly high secretion for liposomes modified with Aqua $\beta$  derivatives having high MGlu% compared with the other liposomes is observed. The results suggest that liposomes modified with Aqua $\beta$  derivatives having high MGlu% activated DCs more effectively than liposomes modified with curdlan derivatives did.

The effect of feeding amounts of  $\beta$ -glucan derivatives to DC2.4 cells was evaluated in the amount of IL-12 secreted from the cells (Fig. 4e). Focusing on MGlu70-Aqua $\beta$ -A6 and MGlu37-Curd-A4, a similar tendency to the relationship

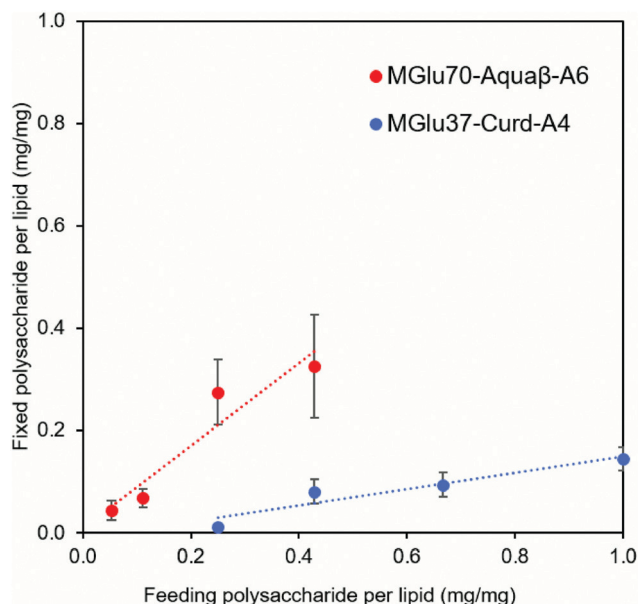


Fig. 2 The modification efficiency of  $\beta$ -glucan derivatives to liposomes. Correlation of modification amounts with feeding amounts of  $\beta$ -glucan derivatives on liposomes was shown. Modification amounts of  $\beta$ -glucan derivatives on liposomes were measured by the phenol-sulfuric acid method. Each point is the mean  $\pm$  SD ( $n = 3$ ).

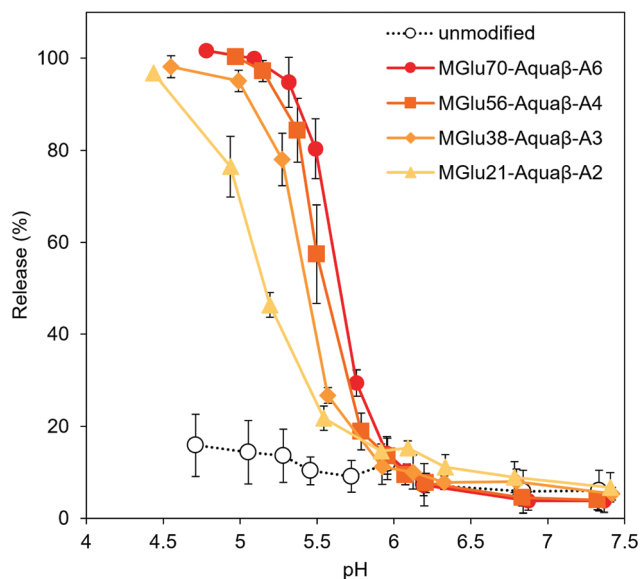


Fig. 3 pH-Sensitivity of liposomes modified with Aqua $\beta$  derivatives. pH-Dependence of pyranine release from liposomes modified with or without Aqua $\beta$  derivatives after 30 min incubation are shown. Lipid concentration was  $2.0 \times 10^{-5}$  M. Each point is the mean  $\pm$  SD ( $n = 3$ ).

between the feeding amount and the fixed amount of  $\beta$ -glucan derivatives to liposomes shown in Fig. 2 was observed. However, in the comparison of  $\beta$ -glucan derivative-modified liposomes with similar amounts of the fixed  $\beta$ -glucan derivatives, Aqua $\beta$  derivative-modified liposomes promoted IL-12 secretion from DC2.4 cells more than curdian derivative-modified liposomes did (Fig. 4e). When  $\beta$ -glucan derivative-modified liposomes were prepared at a feeding rate of 0.11 mg/1 mg lipid of MGLu70-Aqua $\beta$ -A6 and of 0.43 mg/1 mg lipid of MGLu37-Curd-A4, the obtained liposomes showed an identical fixed amount of  $\beta$ -glucan derivatives (Fig. 2). As these  $\beta$ -glucan derivative-modified liposomes were compared, the IL-12 secretion of MGLu70-Aqua $\beta$ -A6-modified liposomes was 10 times higher than that of MGLu37-Curd-A4-modified liposomes (Fig. 4e). Fig. S6 (ESI $^{\dagger}$ ) depicts the correlation between IL-12 production and MGLu group amounts on the liposomes, which is calculated from MGLu% of each  $\beta$ -glucan derivative and its modification amount on the liposomes. In comparison of  $0.08$ – $0.1$  mol mol $^{-1}$  MGLu group amounts per lipid, MGLu70-Aqua $\beta$ -A6-modified liposomes showed much higher IL-12 production from the cells than MGLu37-Curd-A4- and MGLu71-Curd-A6-modified liposomes did, suggesting that a high MGLu density of Aqua $\beta$  derivative-modified liposomes derived from the branching structure of Aqua $\beta$  promoted the activation of DC2.4 cells. These results indicate that Aqua $\beta$  has superior DC activation capability as a backbone of carboxylated polysaccharides to curdian.

Interactions (association and/or uptake) of Aqua $\beta$  derivative-modified liposomes with DC2.4 cells were compared with those of curdian derivative-modified liposomes. DC2.4 cells were treated with fluorescently labeled liposomes, and the fluorescence intensity of the cells was then evaluated using flow cytometry. In the case of Aqua $\beta$  derivative-modified liposomes, all kinds of

liposomes showed higher interactions than unmodified liposomes irrespective of MGLu% (Fig. 5a). On the other hand, the interaction of curdian derivative-modified liposomes with the cells increased with an increase in MGLu% of curdian derivatives. The interaction of liposomes with the cells in the presence of dextran sulfate, which is known to interact with scavenger receptors,<sup>33</sup> was also evaluated in order to discuss the mechanisms of cellular interactions with  $\beta$ -glucan derivative-modified liposomes. Although there was almost no change in fluorescence intensity of the cells treated with MGLu13-Curd-A4- and MGLu37-Curd-A4-modified liposomes even in the presence of dextran sulfate, the cellular interactions of MGLu62-Curd-A4- and MGLu71-Curd-A6-modified liposomes were inhibited by the presence of dextran sulfate (Fig. 5b). This result suggests that MGLu units introduced into curdian in high percentages were recognized by scavenger receptors. Interestingly, the inhibitory effect of dextran sulfate on the interaction of Aqua $\beta$  derivative-modified liposomes with the cells was different from that of curdian derivative-modified liposomes. Dextran sulfate strongly suppressed the interaction of liposomes modified with Aqua $\beta$  derivatives having low MGLu%. However, the cellular interactions of Aqua $\beta$  derivative-modified liposomes in the presence of dextran sulfate was improved with an increase in MGLu%, and MGLu70-Aqua $\beta$ -A6-modified liposomes showed the enhancement of cellular interactions by dextran sulfate (Fig. 5b). These results suggest that the recognition mechanism by DCs differs between curdian derivative- and Aqua $\beta$  derivative-modified liposomes.

### 3.3. Induction of antitumor immunity by Aqua $\beta$ derivative-modified liposomes

Antitumor effects of Aqua $\beta$  derivative-modified liposomes were evaluated using tumor-bearing mice. After OVA-expressing tumor cells (E.G7-OVA cells) were inoculated to mice, OVA-loaded liposomes modified with  $\beta$ -glucan derivatives or PBS were administered subcutaneously to tumor-bearing mice on Days 8 and 14 after tumor inoculation. In the case of mice treated with PBS, tumor volumes increased rapidly and reached endpoints within 30 days (Fig. 6 and Fig. S7, ESI $^{\dagger}$ ). On the other hand, Aqua $\beta$  derivative-modified liposomes suppressed tumor growth in all-treated mice more significantly than PBS (Fig. 6 and Fig. S7, ESI $^{\dagger}$ ). Suppression of tumor growth was not observed in some mice administered with curdian derivative-modified liposomes (Fig. 6 and Fig. S7, ESI $^{\dagger}$ ). This result suggests that Aqua $\beta$  derivative-modified liposomes have a higher therapeutic effect on the E.G7-OVA cancer model than curdian derivative-modified liposomes. After the first injection of the liposomes, some mice showed a mild decrease of body weight (about 5%), but they recovered quickly 2 days after the first injection (Fig. S8, ESI $^{\dagger}$ ). A decline of body weight was not observed after second injection of liposomes. Therefore, toxicities of liposomes are apparently not severe. Aqua $\beta$  derivative-modified liposomes did not show any cytotoxicity to the fibroblast *in vitro* (Fig. S9a, ESI $^{\dagger}$ ), suggesting that these liposomes show no remarkable cytotoxicity to the resident cells at the injection site. We have also investigated antigen-specific immune responses by measuring IFN- $\gamma$  production from splenocytes of the mice immunized with

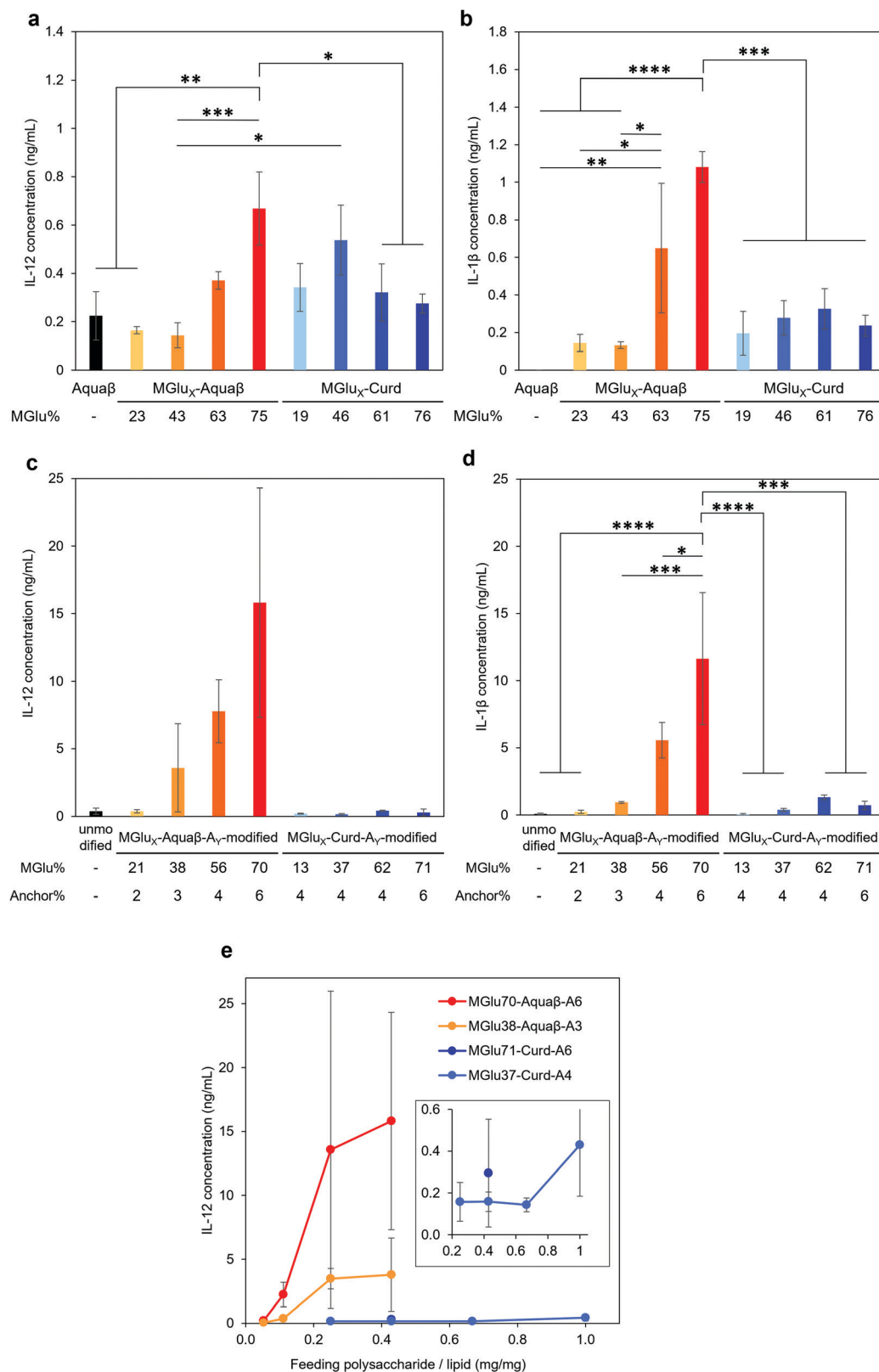


**Fig. 4** Adjuvant properties of  $\beta$ -glucan derivatives and  $\beta$ -glucan derivative-modified liposomes. Cytokine secretion from DC2.4 cells treated with (a, b) Aqua $\beta$  or  $\beta$ -glucan derivatives ( $0.5 \text{ mg mL}^{-1}$ ), or (c, d) unmodified liposomes or liposomes modified with  $\beta$ -glucan derivatives ( $0.4 \text{ mg mL}^{-1}$  lipids) for 24 h. (e) IL-12 production from DC2.4 cells treated with  $\beta$ -glucan derivative-modified liposomes that were prepared with various feeding amounts of  $\beta$ -glucan derivatives. The inset presents an enlarged image for the results of MGlu-Curd-A-modified liposomes. Statistical analyses were conducted using analysis of variance (ANOVA) with Tukey's test. \* $P < 0.05$ ; \*\* $P < 0.01$ ; \*\*\* $P < 0.001$ ; and \*\*\*\* $P < 0.0001$ .

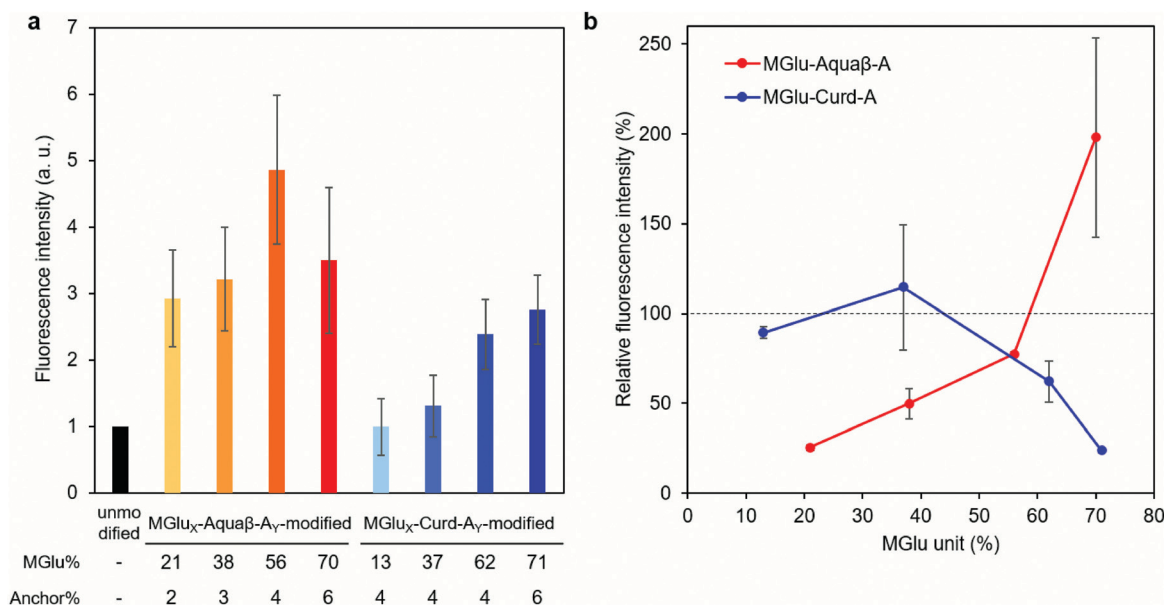


**Fig. 5** Cellular association of liposomes modified with  $\beta$ -glucan derivatives. (a) Fluorescence intensity for DC2.4 cells treated with Dil-labeled liposomes modified with or without  $\beta$ -glucan derivatives for 4 h. (b) DC2.4 cells were treated with Dil-labeled liposomes in the presence of dextran sulfate as an inhibitor of scavenger receptors. The vertical line shows the percentage of fluorescence intensity (FI) with an inhibitor to FI without an inhibitor.

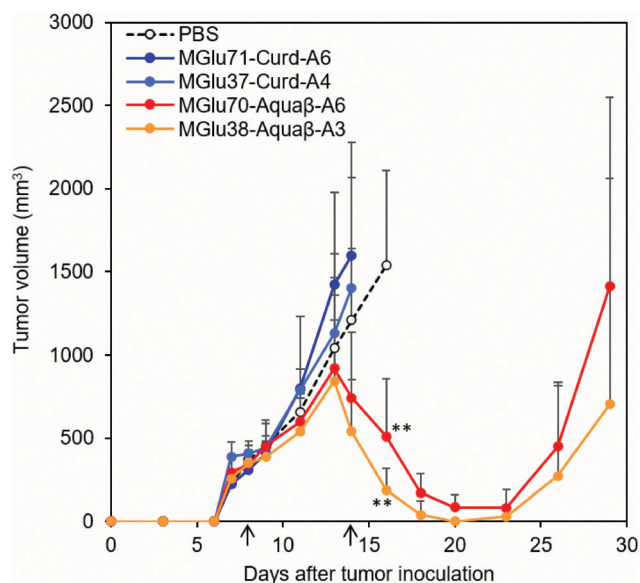


**Fig. 6** Antitumor effects of OVA-loaded liposomes modified with  $\beta$ -glucan derivatives. C57BL/6 mice were immunized on days 8 and 14 after tumor inoculation with PBS or OVA-loaded liposomes modified with  $\beta$ -glucan derivatives. Changes in tumor volume of mice were monitored after inoculation of E.G7-OVA cells ( $5.0 \times 10^5$  cells per mouse). Arrows indicate the days of sample injection. All treated groups included five mice. Statistical analyses comprised analysis of variance (ANOVA) with Tukey's test.  $**P < 0.01$  compared with PBS (on day 16).

OVA-loaded liposomes. As shown in Fig. S9b (ESI<sup>†</sup>), no IFN- $\gamma$  production was detected in the absence of *in vitro* antigen (OVA) stimulation. In contrast, splenocytes of the mice immunized with Aqua $\beta$  derivative-modified liposomes showed significant IFN- $\gamma$

production in the presence of OVA stimulation. These results indicate that Aqua $\beta$  derivative-modified liposomes could induce OVA-specific cellular immune responses, which led the selective cytotoxicity against OVA-expressing tumor cells (E.G7-OVA cells) in the tumor-bearing mice.

### 3.4. Analysis of immune cell composition after immunization of $\beta$ -glucan derivative-modified liposomes

We investigated whether the administration of Aqua $\beta$  derivative-modified liposomes changed the composition of intratumoral immune cells, or not. Since MGLu37-Curd-A4- and MGLu71-Curd-A6-modified liposomes showed an almost identical antitumor effect, MGLu71-Curd-A6-modified liposomes were used as a comparison for Aqua $\beta$  derivative-modified liposomes. Tumors were harvested at 6 days after administration of OVA-loaded liposomes modified with  $\beta$ -glucan derivatives to tumor-bearing mice. The immune cell population in tumors was analyzed using flow cytometry. The frequency of intratumoral CD4<sup>+</sup> T cell population did not change in any of the administered mice, but the frequency of intratumoral CD8<sup>+</sup> T cells increased significantly in mice administered with Aqua $\beta$  derivative-modified liposomes compared with PBS-administered mice (Fig. 7). In addition, the frequency of CD8<sup>+</sup> T cells in mice administered with MGLu38-Aqua $\beta$ -A3-modified liposomes was significantly higher than that in mice administered with MGLu71-Curd-A6-modified liposomes. These results indicate that Aqua $\beta$  derivative-modified liposomes have excellent capability of activating cellular immunity and of promoting the infiltration of CTLs into the tumor.

We next analyzed the intratumoral macrophage population using flow cytometry. The frequency of macrophages expressing MHC-II (M1-phenotype with antitumor character) increased only

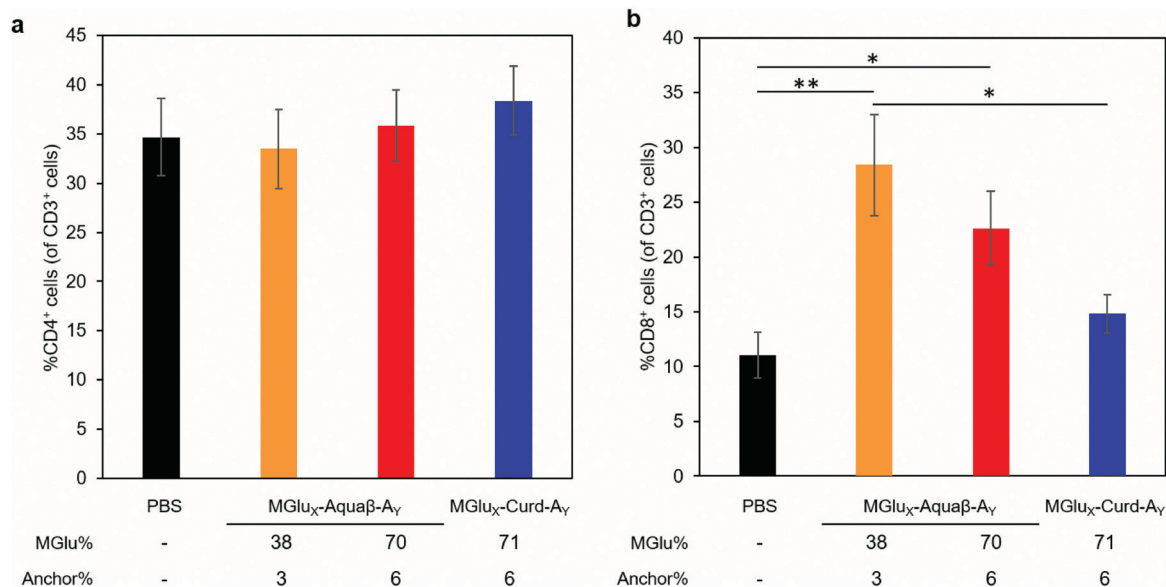


**Fig. 7** T-lymphocyte analysis in a tumor. E.G7-OVA cells were inoculated to C57BL/6 mice. Then PBS or liposomes were subcutaneously immunized to these mice on Day 6. Cell suspension was obtained from tumor on Day 12 followed by flow cytometric analysis. Graphs depict the frequency of (a) CD4<sup>+</sup> cells within CD3<sup>+</sup> T-lymphocytes and (b) CD8<sup>+</sup> cells within CD3<sup>+</sup> T-lymphocytes in live cells of tumor tissue (mean  $\pm$  SEM;  $n = 9$  (PBS), 5 (MGLu38-Aquaβ-A3) and 10 (MGLu70-Aquaβ-A6 and MGLu71-Curd-A6)). Statistical analyses were done using analysis of variance (ANOVA) with Tukey's test. \* $P < 0.05$ ; \*\* $P < 0.01$ .

in mice treated with MGLu38-Aquaβ-A3-modified liposomes (Fig. 8a). The proportion of macrophages expressing CD206 (M2-phenotype with pro-tumor character) tended to decrease more in mice treated with all  $\beta$ -glucan derivative-modified liposomes than in mice treated with PBS. Particularly, the percentage of intratumoral M2 macrophages in mice treated with MGLu70-Aquaβ-A6-modified liposomes was decreased significantly compared with mice treated with PBS (Fig. 8b). The ratio of M1 and M2 macrophages calculated from the results in Fig. 8a and b tended to be higher in Aquaβ derivative-modified liposome-administered mice than PBS-administered mice (Fig. 8c). This result was further confirmed by immunofluorescence staining of the tumor section. As shown by yellow dots in Fig. S10a (ESI<sup>†</sup>), the administration of Aquaβ derivative-modified liposomes tended to increase MHC-II<sup>+</sup> CD11b<sup>+</sup> cells within tumor tissue compared with PBS or MGLu71-Curd-A6-modified liposomes. Furthermore, the administration of all  $\beta$ -glucan derivative-modified liposomes decreased CD206<sup>+</sup> CD11b<sup>+</sup> cells within tumor tissue compared with PBS-treated groups (Fig. S10b, ESI<sup>†</sup>). These results suggest that the administration of Aquaβ derivative-modified liposomes can polarize macrophages in tumors to the tumor-suppressive M1-phenotypes.

## 4. Discussion

Activation of cancer antigen-specific CTLs, more specifically the infiltration of CTLs into tumor tissue, is important for the success of immunotherapy.<sup>2,3</sup> To activate CTLs efficiently, promotion of cross-presentation of antigenic proteins by APC is necessary, as is the activation of APC.<sup>5–7</sup> Cross-presentation is

facilitated primarily by inducing transfer of antigenic proteins to the cytosol of APCs. Antigenic proteins are degraded in the cytosol and are presented on MHC-I molecules as epitope peptides.<sup>5–7</sup> The functional polymers having carboxylated units are protonated in response to weakly acidic pH in endosomes of APCs. The polymer then becomes hydrophobic, which causes membrane fusion or destabilization of liposomes and the endosomal membrane. Therefore, they are often used to promote the transfer of antigenic proteins to the cytosol.<sup>34,35</sup>

To induce antigen-specific immune responses effectively, accumulation of an adjuvant and an antigen in a single carrier, and their simultaneous delivery to APCs are ideal. In our previous study, highly functional antigen carriers were developed by modifying antigen-loaded liposomes with carboxylated curdian derivatives.<sup>24</sup> These liposomes simultaneously achieved an efficient uptake of antigenic proteins by APCs, antigen release into the cytosol, and activation of APCs through innate immunity pathways.<sup>24</sup>

In this study, we sought to improve the immunity-activation ability of liposomes by changing the backbone structure of carboxylated polysaccharides from linear  $\beta$ -glucan (curdian) to branched  $\beta$ -glucan (Aquaβ). Aquaβ was derivatized using a method described previously (Fig. S1, ESI<sup>†</sup>). Modification of  $\beta$ -glucan derivatives to the liposomes was confirmed by zeta potential measurement and the quantification of polysaccharide contents in liposome solution (Fig. 2). Aquaβ derivative-modified liposomes exhibited an identical pH-sensitive content release property with curdian derivative-modified liposomes (Fig. 3, Fig. S4 and S5, ESI<sup>†</sup>). It is particularly interesting that the modification efficiency of Aquaβ derivatives was much higher than that of curdian derivatives (Fig. 2). This difference might be

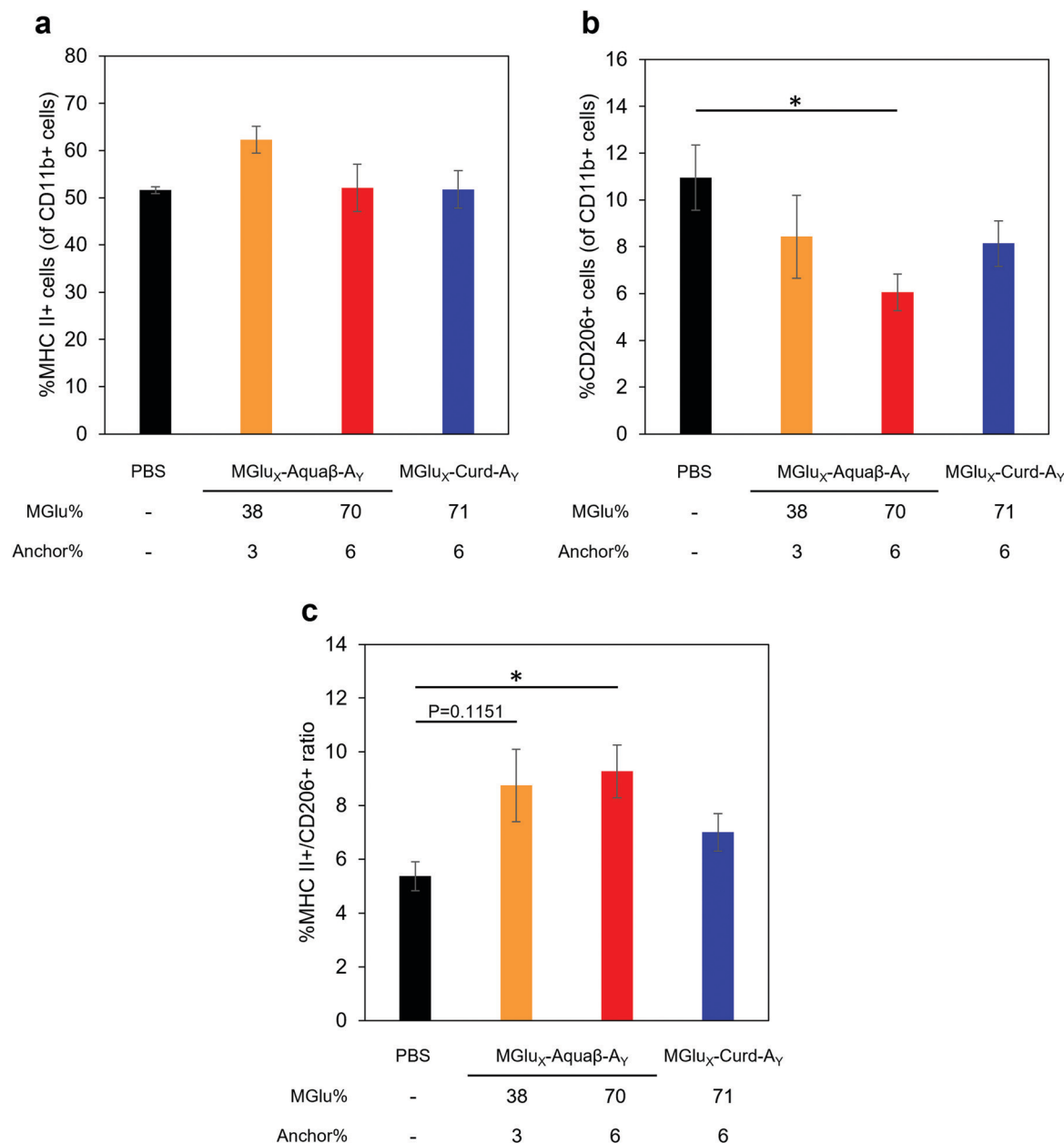


**Fig. 8** Macrophage analysis in a tumor. E.G7-OVA cells were inoculated to C57BL/6 mice. Then PBS or liposomes were immunized subcutaneously to the mice on Day 6. Cell suspension was obtained from tumor on day 12, followed by flow cytometric analysis. Graphs depict the frequency of (a) M1 macrophages (MHC II<sup>+</sup> CD11b<sup>+</sup>), (b) M2 macrophages (CD206<sup>+</sup> CD11b<sup>+</sup>) and (c) M1/M2 ratio (mean  $\pm$  SEM;  $n = 9$  (PBS), 5 (MGLu38-Aquaβ-A3) and 10 (MGLu70-Aquaβ-A6 and MGLu71-Curd-A6)). Statistical analyses were done using analysis of variance (ANOVA) with Tukey's test. \* $P < 0.05$ .

explained from the difference in the anchor density (Table S2, ESI<sup>†</sup>).  $\beta$ -Glucan is known to form a triple helix structure in an aqueous solution,<sup>36,37</sup> whereas our previous data using Congo red suggested that introduction of MGLu units into curdler interfered the triple helix formation of curdler derivatives.<sup>24</sup> Since both of curdler derivatives and Aqua $\beta$  derivatives used in this study might also take random coil structures in an aqueous solution, an increase in the anchor density by introducing anchor groups into branched monosaccharide units of Aqua $\beta$  would increase the possibility of decyl group insertion into the liposomal membrane *via* hydrophobic interactions, resulting in

efficient fixation of Aqua $\beta$  derivatives onto liposomes compared with linear curdler derivatives.

$\beta$ -Glucan derivatives induced secretion of inflammatory cytokines from DC2.4 cells. Their modifications onto liposomes further increased the amounts of secreted cytokines, even though the amounts of  $\beta$ -glucan derivatives added to the cells in later experiments were rather low: the concentrations of  $\beta$ -glucan derivatives in Fig. 4a, b and c, d were calculated as 0.5 mg mL<sup>-1</sup> and 0.06–0.13 mg mL<sup>-1</sup>, respectively. Modification of  $\beta$ -glucan derivatives onto liposomes might exert a multivalent effect of  $\beta$ -glucan derivatives and induce a strong activation

signal *via* receptors on DCs.<sup>38</sup> When compared between liposomes modified with an almost identical amount of curdlan derivatives or Aqua $\beta$  derivatives (Fig. 4e), Aqua $\beta$  derivative-modified liposomes induced cytokine secretion from DCs more effectively than curdlan derivative-modified liposomes did. The results suggest that the backbone structure of  $\beta$ -glucan derivatives affects the adjuvant ability of the  $\beta$ -glucan derivative-modified liposomes. Furthermore, high MGLu density of Aqua $\beta$  derivative-modified liposomes derived from the branching structure of Aqua $\beta$  might also contribute the remarkable activation of DCs (Fig. S6, ESI<sup>†</sup>). Liposomes modified with Aqua $\beta$  derivatives with low MGLu% showed higher cellular association than that of liposomes modified with curdlan derivatives with low MGLu% (Fig. 5a). This might result from high MGLu density of Aqua $\beta$  derivative-modified liposomes compared with curdlan derivative-modified liposomes. The results suggest that conventional curdlan derivative-modified liposomes were taken up mainly *via* scavenger receptors (Fig. 5b), which is consistent with our previous report using curdlan derivative-modified liposomes.<sup>24</sup> The cellular uptake of Aqua $\beta$  derivative-modified liposomes was also fundamentally inhibited by the addition of dextran sulfate, but the effect diminished as the MGLu% of Aqua $\beta$  derivatives increased (Fig. 5b). Surprisingly, in MGLu70-Aqua $\beta$ -A6-modified liposomes, the addition of dextran sulfate promoted intracellular uptake. Taken together, the detailed mechanisms by which the cells recognize Aqua $\beta$  derivatives remain elusive. Additional experiments using other inhibitors for Dectin-1 or TLRs, or knockout of these receptors are necessary to reveal interaction mechanisms between Aqua $\beta$  derivatives and the cells.

In our previous report, administration of curdlan derivative-modified liposomes induced significant suppression of tumor growth.<sup>24</sup> By contrast, in this study, OVA-loaded, curdlan derivative-modified liposomes did not suppress tumor growth in some mice (Fig. S7, ESI<sup>†</sup>). We infer that this is true because we performed liposome administration at a later stage of tumor growth (likely to be more immunosuppressive) than in experiments in our previous report.<sup>24</sup> The average tumor volume at first injection in the current study was  $324 \pm 19.9 \text{ mm}^3$ , which is 6.8 times larger than that of our previous study ( $47.5 \pm 10.8 \text{ mm}^3$ ). In such a later-stage tumor, antitumor immunity induced by curdlan derivative-modified liposomes might not be sufficient to induce significant tumor regression. Even in a late-stage tumor, administration of Aqua $\beta$  derivative-modified liposomes significantly suppressed the growth of large E.G7-OVA tumors in all mice compared with PBS and curdlan derivative-modified liposomes (Fig. 6 and Fig. S7, ESI<sup>†</sup>). After subcutaneous injection, Aqua $\beta$  derivative-modified liposomes that have high modification efficiency of polysaccharide derivatives might be taken up by APCs and promote inflammatory cytokine secretions from these cells, which resulted in effective activation of antitumor cellular immune responses compared with curdlan derivative-modified liposomes. CD8<sup>+</sup> T cells induced by immunization of Aqua $\beta$  derivative-modified liposomes migrated to the tumor tissue effectively (Fig. 7b), which contributed the significant

suppression of tumor growth directly. Macrophages in a tumor are polarized to the tumor-suppressive M1-phenotype by stimulation with IFN- $\gamma$ .<sup>39,40</sup> Consequently, IFN- $\gamma$  secretion from CD8<sup>+</sup> T cells infiltrated to the tumor might also induce the polarization of tumor-associated macrophages to M1-phenotypes and increase the M1/M2 ratio in the tumor (Fig. 8 and Fig. S10, ESI<sup>†</sup>), which canceled immunosuppression within tumor and assisted suppression of tumor growth in the treatment of Aqua $\beta$  derivative-modified liposomes.

## 5. Conclusions

For this study, carboxylated Aqua $\beta$  derivatives, which have a branched structure as a backbone, were synthesized to enhance the antitumor efficacy of antigen-loaded liposomes. The modification efficiency of Aqua $\beta$  derivatives to the liposomes was significantly higher than that of conventional curdlan derivatives. Aqua $\beta$  derivative-modified liposomes released their cargo in response to weakly acidic pH, which corresponds to an endosomal/lysosomal environment. OVA-loaded, Aqua $\beta$  derivative-modified liposomes interacted effectively with a DC cell line and induced secretion of inflammatory cytokines. Furthermore, the liposomes increased the percentage of intratumoral CD8<sup>+</sup> T cells and polarized intratumoral macrophages to the M1-phenotype, resulting in significant growth suppression of large E.G7-OVA tumor in mice. The results obtained from this study underscore the importance of the selection of the backbone structure to induce strong cellular immunity and to obtain enhanced therapeutic effects. The results demonstrate that Aqua $\beta$  derivative-modified liposomes can be promising materials for liposomal vaccines to achieve efficient delivery of antigens, activation of DCs and antigen-specific immunity.

## Author contributions

Shin Yanagihara: data curation, formal analysis, investigation, methodology, writing – original draft, Nozomi Kasho: data curation, formal analysis, investigation, methodology, Koichi Sasaki: data curation, formal analysis, investigation, methodology, writing – original draft, Naoto Shironaka: investigation, methodology, Yukiya Kitayama: data curation, formal analysis, writing – review & editing, Eiji Yuba: conceptualization, data curation, formal analysis, funding acquisition, investigation, methodology, project administration, supervision, validation, writing – original draft, writing – review & editing, Atsushi Harada: data curation, formal analysis, project administration, supervision, validation, writing – review & editing.

## Conflicts of interest

There are no conflicts to declare.

## Acknowledgements

This research was funded by the Grants-in-aid for Scientific Research from the Ministry of Education, Science, Sports, and

Culture in Japan (grant number 15H03024). The authors thank Takumi Tsujimura and Misaki Kitagawa (Osaka Prefecture University) for their kind support in animal experiments. The authors appreciate Dr Maki Ohashi (Sanyo Fine Co., Ltd) for his kind support for Aquaß providing.

## References

- 1 S. Khan and D. E. Gerber, *Semin. Cancer Biol.*, 2020, **64**, 93–101.
- 2 R. Khazen, S. Müller, F. Lafouresse, S. Valitutti and S. Cussat-Blanc, *Sci. Rep.*, 2019, **9**, 1208.
- 3 N. Varadarajan, B. Julg, Y. J. Yamanaka, H. Chen, A. O. Ogguniyi, E. McAndrew, L. C. Porter, A. Piechocka-Trocha, B. J. Hill, D. C. Douek, F. Pereyra, B. D. Walker and J. C. Love, *J. Clin. Invest.*, 2011, **121**, 4322–4331.
- 4 S. Rosenberg, J. Yang and N. Restifo, *Nat. Med.*, 2004, **10**, 909–915.
- 5 N. I. Ho, L. G. M. Huis in 't Veld, T. K. Raaijmakers and G. J. Adema, *Front. Immunol.*, 2018, **9**, 2874.
- 6 A. Rodriguez, A. Regnault, M. Kleijmeer, P. Ricciardi-Castagnoli and S. Amigorena, *Nat. Cell Biol.*, 1999, **1**, 362–368.
- 7 O. Joffre, E. Segura, A. Savina and S. Amigorena, *Nat. Rev. Immunol.*, 2012, **12**, 557–569.
- 8 S. Burgdorf, A. Kautz, V. Bohnert, P. A. Knolle and C. Kurts, *Science*, 2007, **316**, 612–616.
- 9 A. Ahmad, J. M. Khan and S. Haque, *Biochimie*, 2019, **160**, 61–75.
- 10 J. Zepeda-Cervantes, J. O. Ramírez-Jarquín and L. Vaca, *Front. Immunol.*, 2020, **11**, 1100.
- 11 J. Sheen, M. G. Strainic, J. Liu, W. Zhang, Z. Yi, M. E. Medof and P. S. Heeger, *J. Immunol.*, 2017, **199**, 278–291.
- 12 S. Saijo, N. Fujikado, T. Furuta, S. Chung, H. Kotaki, K. Seki, K. Sudo, S. Akira, Y. Adachi, N. Ohno, T. Kinjo, K. Nakamura, K. Kawakami and Y. Iwakura, *Nat. Immunol.*, 2007, **8**, 39–46.
- 13 P. R. Taylor, D. M. Reid, S. Heinsbroek, G. D. Brown, S. Gordon and S. Wong, *Eur. J. Immunol.*, 2005, **35**, 2163–2174.
- 14 C. Zilker, D. Kozlova, V. Sokolova, H. Yan, M. Eppele, K. Überla and V. Temchura, *Nanomedicine*, 2017, **13**, 173–182.
- 15 X. Dong, J. Liang, A. Yang, Z. Qian, D. Kong and F. Lv, *ACS Appl. Mater. Interfaces*, 2019, **11**, 4876–4888.
- 16 F. Aosai, M. S. Rodriguez Pena, H. S. Mun, H. Fang, T. Mitsunaga, K. Norose, H. K. Kang, Y. S. Bae and A. Yano, *Cell Stress Chaperones*, 2006, **11**, 13–22.
- 17 J. Banachereau and R. Steinman, *Nature*, 1998, **392**, 245–252.
- 18 E. Yuba, C. Kojima, A. Harada, Tana, S. Watarai and K. Kono, *Biomaterials*, 2010, **31**, 943–951.
- 19 E. Yuba, A. Harada, Y. Sakanishi and K. Kono, *J. Controlled Release*, 2011, **149**, 72–80.
- 20 E. Yuba, N. Tajima, Y. Yoshizaki, A. Harada, H. Hayashi and K. Kono, *Biomaterials*, 2014, **35**, 3091–3101.
- 21 M. Okubo, M. Miyazaki, E. Yuba and A. Harada, *Bioconjugate Chem.*, 2019, **30**, 1518–1529.
- 22 S. Saijo, N. Fujikado, T. Furuta, S. Chung, H. Kotaki, K. Seki, K. Sudo, S. Akira, Y. Adachi, N. Ohno, T. Kinjo, K. Nakamura, K. Kawakami and Y. Iwakura, *Nat. Immunol.*, 2007, **8**, 39–46.
- 23 H. L. Rosenzweig, J. S. Clowers, G. Nunez, J. T. Rosenbaum and M. P. Davey, *Inflammation Res.*, 2011, **60**, 705–714.
- 24 E. Yuba, A. Yamaguchi, Y. Yoshizaki, A. Harada and K. Kono, *Biomaterials*, 2017, **120**, 32–45.
- 25 H. Kono, N. Kondo, K. Hirabayashi, M. Ogata, K. Totani, S. Ikematsu and M. Osada, *Carbohydr. Polym.*, 2017, **174**, 876–886.
- 26 D. Muramatsu, K. Kawata, S. Aoki, H. Uchiyama, M. Okabe, T. Miyazaki, H. Kida and A. Iwai, *Sci. Rep.*, 2014, **4**, 777.
- 27 D. Fujikura, D. Muramatsu, K. Toyamane, K. Toyomae, S. Chiba, T. Daito, A. Iwai, T. Kouwaki, M. Okamoto, H. Higashi, H. Kida and H. Oshiumi, *J. Biochem.*, 2018, **163**, 31–38.
- 28 Y. Kimura, M. Sumiyoshi, T. Suzuki, T. Suzuki and M. Sakanaka, *Int. Immunopharmacol.*, 2007, **7**, 963–972.
- 29 I. Popescu, I. M. Pelin, G. L. Ailiesei, D. L. Ichim and D. M. Suflet, *Carbohydr. Polym.*, 2019, **224**, 115157.
- 30 *Food Analysis Laboratory Manual. Food Science Text Series*, ed. S. S. Nielsen, *Springer, Cham*, 2017, pp. 137–142.
- 31 T. Masuko, A. Minami, N. Iwasaki, T. Majima, S. Nishimura and Y. C. Lee, *Anal. Biochem.*, 2005, **339**, 69–72.
- 32 Y. Yoshizaki, E. Yuba, N. Sakaguchi, K. Koiwai, A. Harada and K. Kono, *Biomaterials*, 2017, **141**, 272–283.
- 33 N. Platt, H. Suzuki, Y. Kurihara, T. Kodama and S. Gordon, *Proc. Natl. Acad. Sci. U. S. A.*, 1996, **93**, 12456–12460.
- 34 M. A. Aghdam, R. Bagheri, J. Mosafer, B. Baradaran, M. Hashemzaei, A. Baghbanzadeh, M. de la Guardia and A. Mokhtarzadeh, *J. Controlled Release*, 2019, **315**, 1–22.
- 35 E. Yuba, *J. Mater. Chem. B*, 2020, **8**, 1093.
- 36 K. Miyoshi, K. Uezu, K. Sakurai and S. Shinkai, *Chem. Biodiversity*, 2004, **1**, 916–924.
- 37 H. Kono, N. Kondo, T. Isono, M. Ogata and K. Hirabayashi, *Int. J. Biol. Macromol.*, 2020, **154**, 1382–1391.
- 38 H. Duan, M. Donovan, A. Foucher, X. Schultze and S. Lecommandoux, *Sci. Rep.*, 2018, **8**, 14730.
- 39 R. D. Stout, C. Jiang, B. Matta, I. Tietzel, S. K. Watkins and J. Suttles, *J. Immunol.*, 2005, **175**, 342–349.
- 40 K. J. Mylonas, M. G. Nair, L. Prieto-Lafuente, D. Paape and J. E. Allen, *J. Immunol.*, 2009, **182**, 3084–3094.